BAE Systems Charge Coupled Device Radiation Test Results

Michael R. Jones[1]
Ronald Schrein[2]
William Koldewyn[2]
Marco Sirianni[3]
Paul Vu[4]
Paul W. Marshall[5]

1. NASA/Orbital Sciences Corporation
2. Ball Aerospace and Technologies Corporation
3. Johns Hopkins University, Department of Physics and Astronomy
4. BAE Systems
5. Consultant

DUT: BAE Systems/Fairchild CCD486 Charge-Coupled Device, S/N 3188
Date: 9 March 2001
Facility: University of California at Davis Crocker Nuclear Laboratory (UCD/CNL) Cyclotron
Test: Displacement damage, 63 MeV protons

1. Introduction

The Hubble Space Telescope Advanced Camera for Surveys (ACS) instrument will employ a large format Charge-Coupled Device (CCD) detector in the Wide Field Channel (WFC) imaging camera. HST flies in a 28.5° inclination 600 km nominal orbit that will expose the WFC CCD detector to high-energy protons in the South Atlantic Anomaly (SAA). Flight data from the HST Space Telescope Imaging Spectrograph (STIS) and Wide Field/Planetary Camera II (WFPC2) show that proton displacement damage has measurably degraded the charge-transfer efficiency (CTE) of the CCD detectors in those instruments. CTE degradation causes error in stellar photometry and distortion in the observed surface brightness of extended objects.

At the request of the HST program, proton testing was performed to assess the degradation of the BAE Systems CCD486 CCD caused by displacement damage. A custom 2k x 4k butted CCD imager from Scientific Imaging Technologies, Incorporated (SITe) was the baseline detector for the ACS WFC camera. The purpose of the test was to determine whether the CCD486 would be a suitable substitute for the SITe imager. Features of the CCD486 are summarized in Table 1.

Imaging Area Format	4096 x 4096
Pixel Pitch Size	15μ x 15μ
Serial Registers	2
Output Amplifiers	4
Mini-Channel	3μ, parallel and serial registers
Processing	buried n-channel, thinned, back illuminated
AR Coating	Lesser Cu red
Clocking	3-phase
Rated Readout Noise	<4 e^- rms @ 50kpix/sec
Rated Full-Well	100 ke^- MPP*, 400 ke^- non-MPP
Rated Dark Current @ 25° C	25.0 pA/cm^2 MPP, 2.0 nA/cm^2 non-MPP

*Multi-Pinned Phase

Table 1. BAE Systems CCD486 CCD specifications.

The imager is segmented into four quadrants that can be independently clocked to enable vertical register split-frame readout through the two serial registers. Each serial register is split into two halves to allow horizontal split-frame readout.

2. Test Conditions

Two different regions of the CCD were irradiated with 63 MeV protons to fluences of 2.5×10^9 p/cm^2 and 5×10^9 p/cm^2. TID was ~340 rad (Si) and ~680 rad (Si), respectively, for the 2.5×10^9 p/cm^2 and 5×10^9p/cm^2 exposures. The 63 MeV fluences were chosen to approximate the NIEL equivalent proton DDD at 2.5 and 5 years in the HST natural radiation environment[1]. Irradiation was carried out at room temperature with the imager unbiased.

Incremental exposure of two vertical (column-aligned) sections of the imager was achieved by using a movable 2 cm thick aluminum mask. The CCD was mounted in a specially designed fixture fitted with alignment dowels for the mask. Figure 1 shows the fixture with the imager oriented such that the columns are horizontal. Ribbon cables for the clocks, biases and outputs of the four quadrants (unused during the test) are attached to the CCD carrier.

To improve the uniformity of the coverage, the long axis of the unmasked area of the imager was tilted 60° relative to the beam and centered in front of the beam exit window. Beam uniformity across the projected unmasked area of the imager was measured by exposing radiographic film mounted in the test fixture. Manual densitometry measurements performed at Davis indicate that the exposure of the unmasked (60° tilted) area of the CCD was uniform to better than ~20%. The aluminum mask was actually 1 cm thick, but the initial radiographic films revealed hot spots coinciding with the holes drilled into the mask for the alignment dowels. To eliminate the hot spots, a second spare 1 cm thick mask was placed in front of the first mask, as shown in Figure 1.

For the 2.5×10^9 p/cm^2 exposure, the mask edge was offset by ~500 columns to one side of the vertical center split. The 5×10^9 p/cm^2 exposure was achieved by moving the mask to shield the 2.5×10^9 p/cm^2 section of the CCD. Offset of the mask was required to ensure that scattering of primary and secondary particles at the edge would not affect serial First Pixel Response (FPR) measurements for the 2.5×10^9 p/cm^2 exposure.

Pre- and post-rad measurements were performed in the Ball Aerospace and Technologies Corporation (BATC) ACS CCD characterization laboratory. Experimental conditions for the measurements are shown in Table 2.

Surface dark current was suppressed by operating the imager in inverted MPP mode. The MPP boron implant in the CCD486 is under parallel phase 3, hence the offset in the P3 clock rails relative to P1 and P2 in Table 2.

3. Parallel CTE

Parallel CTE was measured using the ^{55}Fe x-ray stimulation and FPR techniques[2]. ^{55}Fe Kα x-rays (5.9 keV) produce a charge packet of known size, 1620 electrons, in silicon. The signal loss in the charge packet as a function of the number of transfers (row or column) yields the CTE. Gain calibration of the CCD output amplifier and signal processing chain was derived by extrapolating the ^{55}Fe Kα line in the 'stacking plot' to zero transfers.

---

[1] Jones, Michael R., *ACS WFC CCD Radiation Test: The Radiation Environment*, Space Telescope Science Institute Instrument Science Report 00-09, 15 May 2000.

[2] Waczynski, Augustyn, et al., *A Comparison of Charge Transfer Efficiency Measurements Techniques on Proton Damaged n-Channel CCDs for the Hubble Space Telescope Wide-Field Camera 3*, IEEE Trans. Nuc. Sci., Vol. 48, No. 6, December 2001.

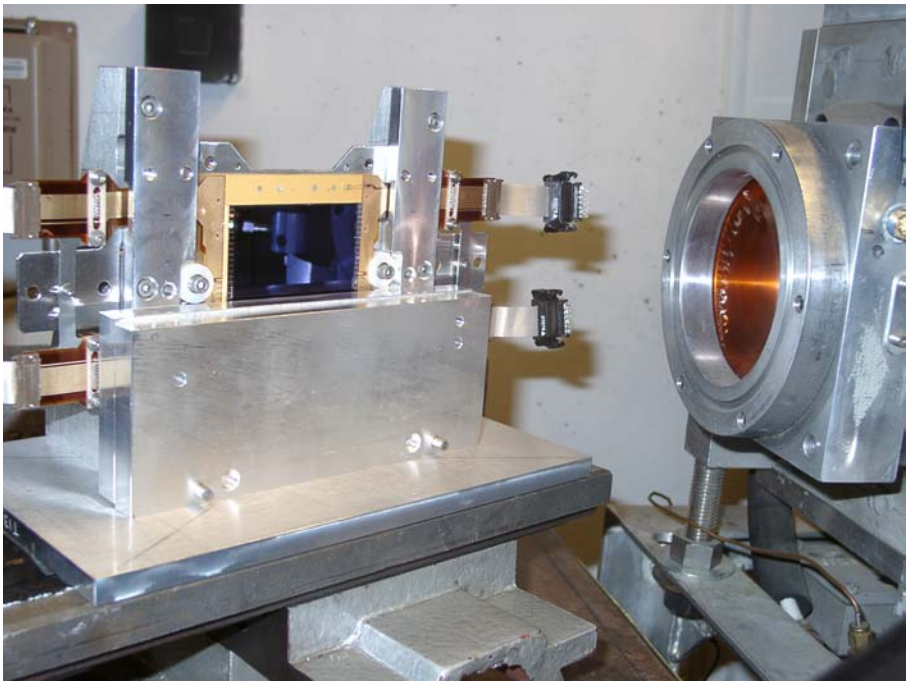

Figure 1. Test fixture for the BAE CCD486 proton test.

Temperature	-81 °C
Phase 1, Phase 2 Vertical Rails	+2 V, -8 V
Phase 3 Vertical Rails	+4 V, -6 V
Vertical Transfer Gate	+5 V, -6 V
Horizontal Rails	+6 V, -4 V
Output Summing Gate	+4 V, -4 V
Reset Gate	+8 V, 0 V
V_{rd}	+15.5 V
V_{dd}	+23.5 V
Parallel Transfer	640 μsec/row excluding serial readout time
Serial Transfer	22 μsec/pix
Serial Clock Edge Rise Time	~200 nsec
Parallel Clock Edge Rise Time	~1 μsec

Table 2. Experimental parameters for CCD486 characterization.

CTE is measured in the FPR technique from the signal loss experienced in the leading row (or column) of an electronically formed knife-edge in a flat lamp image. It was for the FPR test that we exploited the segmented architecture of the CCD486. The knife-edge was generated by clocking two of the quadrants to flush out the flat lamp signal while holding the clocks static in the other two quadrants to retain half of the flat image. After the half frame flush, the full frame was read out with normal timing.

Figure 2 shows the parallel CTE and charge transfer inefficiency (CTI=1-CTE) results. As observed in previous tests, ^{55}Fe and FPR are in good agreement. CTI exhibits simple power law behavior except for an apparent break in the slope of the $5x10^9$ p/cm^2 curve at signal levels <100 electrons. The cause of the change in the slope of the $5x10^9$ p/cm^2 CTE measurement at low signal levels is unclear.

Pre-rad parallel CTE at 1620 electrons was 0.999999 per pixel. After a DDD of $8.8x10^6$ MeV/g ($2.5x10^9$ p/cm^2 @ 63 MeV), the ^{55}Fe CTE dropped to 0.999924/pixel (CTI=$7.6x10^{-5}$/pixel) with power law FPR CTE behavior at other signal levels. Note that though the per-pixel CTE remains above 0.9999, the

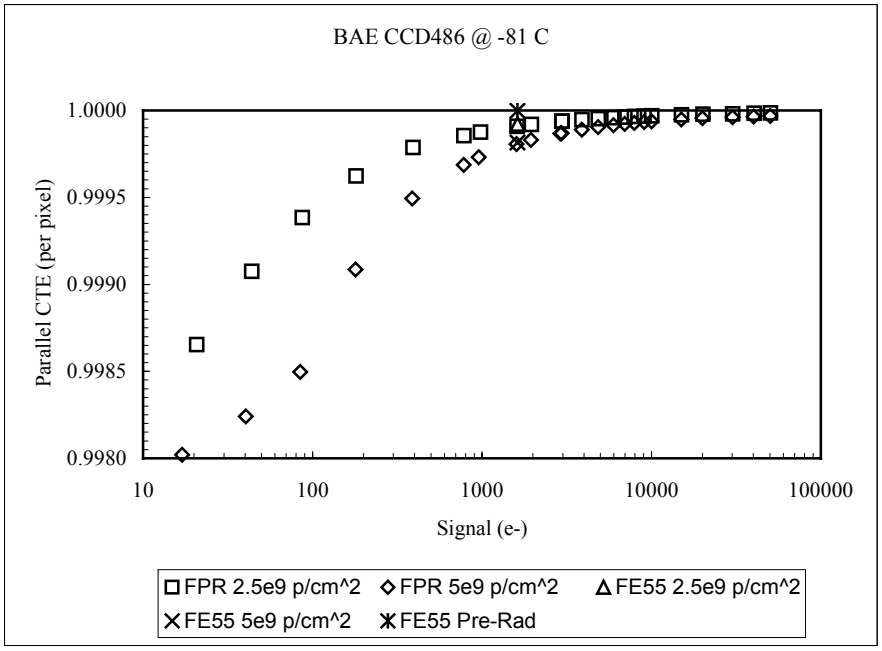

(a)

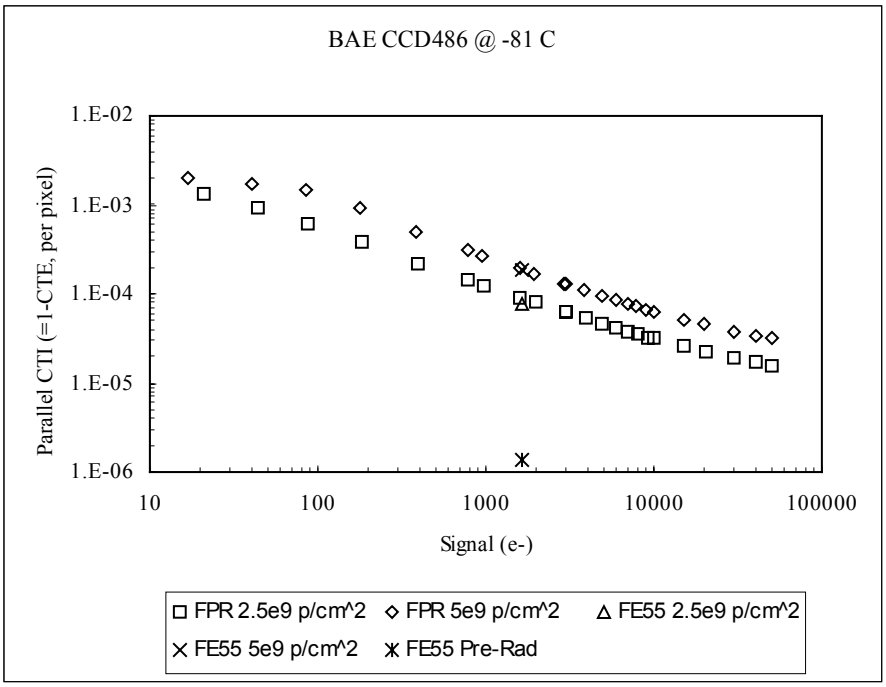

(b)

Figure 2. BAE CCD486 radiation test results: (a) parallel CTE, (b) parallel CTI.

potential impact for low brightness science targets against a dark background is not insignificant. In the worst case of 4096 parallel transfers, a CTE of 0.999924/pixels represents a signal loss at 1620 electrons of roughly 27% ($1-0.999924^{4096}$). Operating the imager in split-frame mode to reduce the maximum number of vertical transfers to 2048 still results in a signal loss of ~14%. The power law extrapolation to lower signal levels below 1620 electrons implied by the FPR curve suggests even more severe charge transfer related signal loss in faint targets.

Parallel ^{55}Fe CTE decreased to 0.99982/pixel (CTI=$1.8\text{x}10^{-4}$/pixel) for a fluence of $5\text{x}10^9$ p/cm^2. The ratio of the FPR $5\text{x}10^9$ p/cm^2 CTI curve to the $2.5\text{x}10^9$ p/cm^2 CTI curve varied from ~1.5 to ~2.4. Over a restricted signal range of ~800-50,000 electrons, the measured ratio is between 2.0 and 2.2. This result suggests that the parallel CTI scales linearly with the proton fluence and therefore with the proton displacement damage. For 2048 and 4096 vertical transfers, 0.99982/pixel CTE would result ~31% and ~52% loss of charge for a signal of 1620 electrons, respectively. The monotonic decrease in CTE at lower signal levels implied by FPR suggests severe image degradation for faint science targets against a dark background.

4. Serial CTE

Serial CTE was also measured with the ^{55}Fe and FPR methods. In serial FPR, a vertical knife-edge is formed by clocking one half of the horizontal register while holding the clocks for the other half static. Offsetting the mask edge to one side of the vertical quadrant boundary ensured that damage due to scattered particles would not compromise the knife-edge in the FPR test. The reference signal level for the $2.5\text{x}10^9$ p/cm^2 measurement was estimated from the 500 columns of the flat between the edge of the mask and the center split.

Figure 3 shows the serial CTE and CTI measurements for $2.5\text{x}10^9$ p/cm^2. Serial FPR data was also taken by reading out the half-flat through the amplifier on the $5\text{x}10^9$ p/cm^2 side of the imager. The $5\text{x}10^9$ p/cm^2 data is not considered reliable, however, because during line read the FPR knife-edge was first clocked through the 500 pixels exposed at $2.5\text{x}10^9$ p/cm^2 and through the pixels damaged by scattering at the edge of the mask. Agreement between ^{55}Fe and FPR is not a close as in the parallel CTE test, but the uncertainty in the serial ^{55}Fe measurement is likely to be large. We have found that post-rad serial ^{55}Fe is, in general, difficult to measure accurately because the Kα single-pixel event line is faint and broad.

Figure 4 compares the parallel and serial FPR CTI for $2.5\text{x}10^9$ p/cm^2. Serial CTE is higher than parallel CTE (serial CTI is lower than parallel CTI) at all signal levels. We have found the same qualitative trend in assessment of other imagers for the ACS CCD radiation test program. Based on this data, we can expect that on-orbit charge loss effects will be observed primarily in the vertical transfer direction.

The comparison between horizontal and vertical CTE also has important implications for mini-channel effectiveness in the BAE CCD486. In Figure 3 (a) the serial CTE exhibits a clear S-shaped signature beginning at a signal level of ~7000 electrons. Our physical interpretation of this 'bump' in the serial CTE curve is that it represents the charge capacity of the 3µ supplemental implant in the horizontal register. At lower signal levels, the charge packet is confined to the mini-channel. At high signal levels, the charge packet overflows the mini-channel and expands into the main n-channel. The CTE decreases because a larger number of traps are contained within the expanded volume of the charge packet. The contrast between the effectiveness of the mini-channel implant in the horizontal register and in the vertical registers is striking. There is no evidence of a mini-channel signature in the parallel FPR curve. The vertical register 3µ mini-channel implant appears to provide no radiation hardness benefit at low signal levels, at least for the biases, clock rails, and readout timing used for this test.

5. Discussion

We have made simplistic estimates of low signal level charge loss based on the parallel CTE measurements that do not adequately reflect the true impact on the science data. Charge in the original signal packet that is captured in traps during transfer is not permanently lost, but instead reappears at a later time in a trailing pixel. Thus, our signal loss estimates are more correctly interpreted to mean that a percentage of the

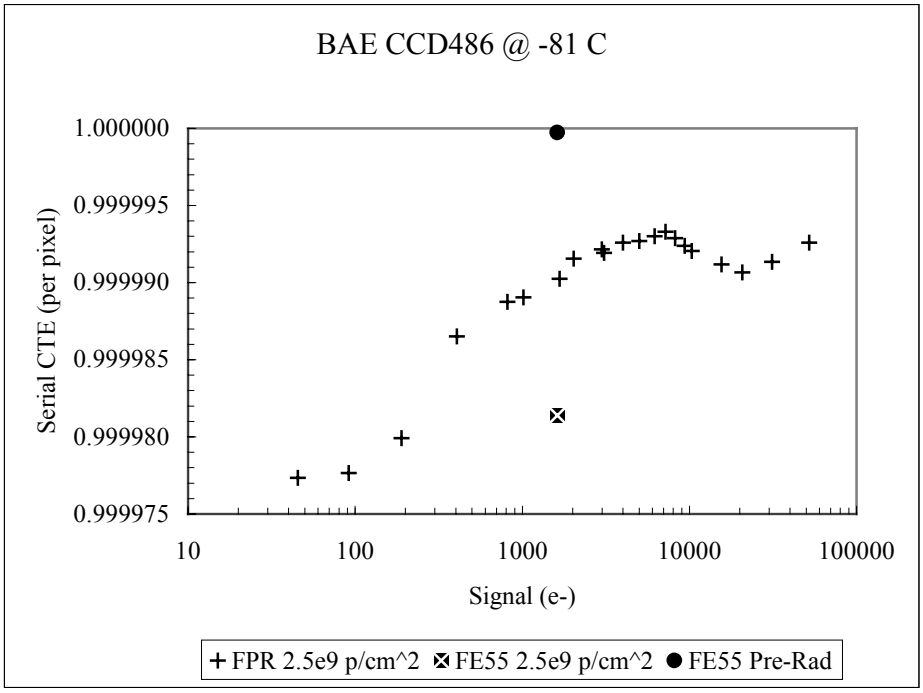

(a)

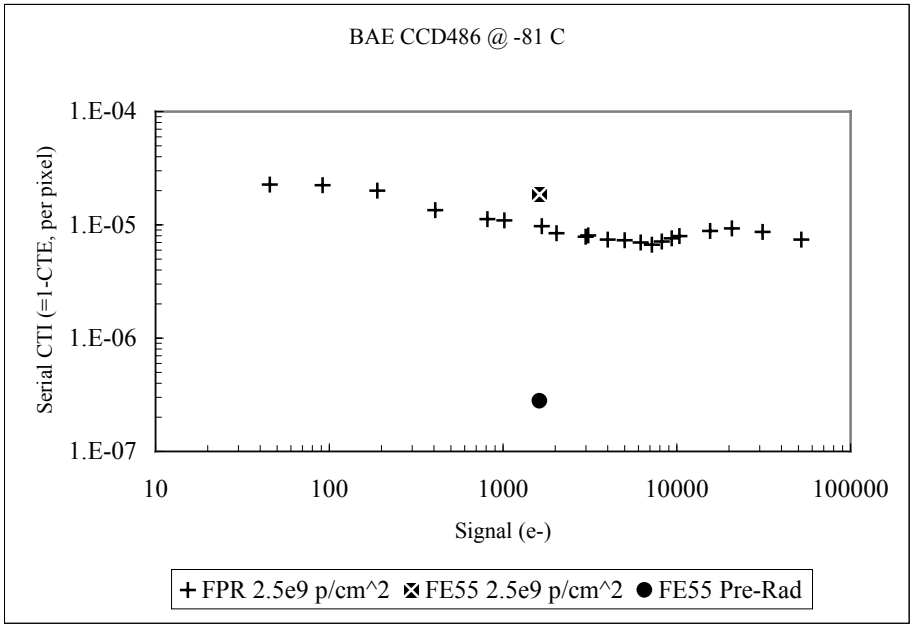

(b)

Figure 3. BAE CCD486 radiation test results: (a) serial CTE, (b) serial CTI.

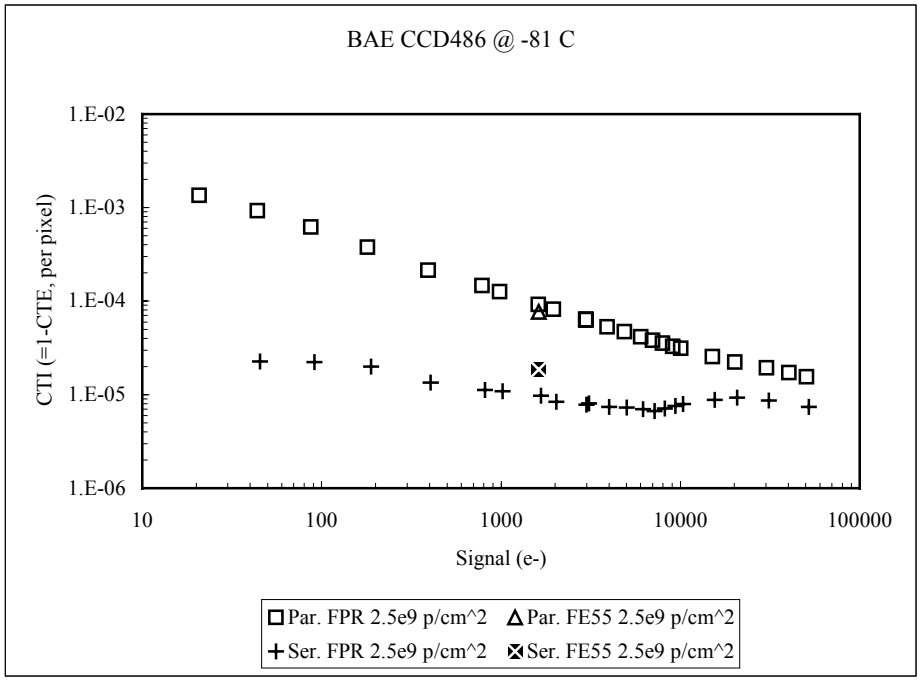

Figure 4. Comparison of 2.5×10^9 p/cm^2 FPR CTI.

carriers contained in the original charge packet are redistributed in the trailing pixel (or pixels). Furthermore, the FPR and ^{55}Fe techniques tend to yield a conservative measure of CTE because the signal packet is clocked through pixels containing little or no charge. We have not investigated the effect of background charge (or 'fat-zero') in this test, but it is known that CTE can be improved if the traps are pre-filled with carriers before readout begins. The background can arise unintentionally through the accumulation of dark current or the generation of spurious charge or it could be the result of integration of low-level light in the science image. Background charge can also be intentionally introduced by pre- or post-flashing the image with a flat field before readout. FPR is a conservative CTE measurement by design since the preceding half of the flat is flushed before the knife-edge is clocked out. ^{55}Fe is conservative and correlates well with FPR so long as the x-ray density is low enough that partial x-ray events and deferred charge from single-pixel events does not form an unintentional fat-zero.

A rigorous quantitative assessment of the science impact of the CTE degradation measured in this test would require a modeling approach beyond the scope of this work. A generally accepted and practical modeling strategy that correctly accounts for the complexity of CCD charge transfer remains elusive despite ongoing efforts in the community to develop such a tool. We can nevertheless understand the qualitative implications for science. In stellar photometry, charge deferral induces photometric error because captured charge that reappears outside the sampling window (synthetic aperture) is not measured. Precision stellar astrometry is also impacted. Imperfect CTE causes redistribution of the signal in the star image. The PSF of the star is distorted, resulting in shift of the observed centroid in both the x and y directions relative to the true centroid. As with photometric error, centroid error will increase with time as displacement damage builds-up in the CCD. Our measurements show that vertical CTE is more severely degraded than horizontal CTE, which indicates that we can expect the radiation induced y-centroid (vertical) astrometric error to be greater than the x-centroid (horizontal) astrometric error. Degraded charge transfer will alter the observed brightness distribution of extended resolved targets (e.g. galaxies). A fraction of the charge in the leading edge of the image (in both directions) will be captured in traps and be released during readout into the following rows or columns of the image. The redistribution of signal will lead to deviations between the measured surface brightness and true surface brightness of the target.

Although our rough calculations of charge loss/redistribution lack rigor, orbital data from WFPC2 and STIS supports our conclusion that radiation damage will measurably degrade the ACS WFC science images. Error in WFPC2 stellar photometric measurements has increased steadily since the instrument was installed in December 1993 (HST Servicing Mission 1). As of August 2000, the worst-case error for a faint star against a dark background was 52%[3]. The STIS CCD detector has also degraded since launch (February 1997). Low signal level, dark background ('sparse field') photometric error was ~6% after 0.9 years on-orbit, increasing to ~29% after 2.6 years[4][5]. In WFPC2, a study of galaxy images has shown that signal redistribution caused by degraded charge transfer introduces false asymmetry in the galaxy surface brightness profiles[6].

6. Summary

A BAE CCD486 charge-coupled device has been exposed to 63 MeV proton fluences of 2.5×10^9 p/cm^2 and 5×10^9 p/cm^2. These proton fluences roughly approximate the predicted displacement damage in the HST ACS WFC CCD imager after 2.5 and 5 years in the natural space radiation environment. Parallel CTE at a signal level of 1620 electrons (^{55}Fe) degraded from 0.999999 pre-rad to 0.999924 after 2.5×10^9 p/cm^2. FPR measurements above and below 1620 electrons show power-law CTE variation as a function of signal level. CTI increased by a factor of ~2 from 2.5×10^9 p/cm^2 to 5×10^9 p/cm^2 over most of the signal range covered by the measurements. This result suggests that the CTI scales with displacement damage, at least up to a NIEL equivalent 63 MeV proton fluence of 5×10^9 p/cm^2. Assuming our environment modeling and transport calculations are accurate, the ground test data predicts that the CTI increase during the first 5 years on-orbit will be proportional to the accumulated trapped proton fluence (taking into account the solar cycle dependence of the proton flux). We cannot predict from this dataset whether the CTI will continue to be proportional to proton exposure beyond a fluence of 5×10^9 p/cm^2. Significant uncertainties exist in the predicted mapping (at least a factor of 2 and possibly greater) between time on-orbit and the 63 MeV proton fluences utilized in the test. There is at present no practical methodology to reduce the uncertainties because the correlation between ground test measurements and on-orbit experience has not been studied either for WFPC2 or STIS.

Serial CTE was superior to parallel CTE at all signal levels in the 2.5×10^9 p/cm^2 test. FPR indicates that the 3μ mini-channel implant in the horizontal register provides a radiation hardness advantage at low signal levels when flight clock patterns are used to read out the CCD. The overflow capacity of the horizontal mini-channel is ~10,000 electrons. The vertical register mini-channel implant does not appear to function as intended; there is no evidence in the parallel FPR data of an S-shaped signature similar to that seen in the serial data. This is an unfortunate result since our data shows that parallel charge transfer is more severely degraded by radiation damage than serial charge transfer. Because we have not modeled charge transfer in the CCD486, we can only speculate about the cause of the dramatically different behavior of the horizontal and vertical mini-channel implants. We suggest that a carrier confined in the mini-channel 'notch' has a characteristic time constant for escape from the mini-channel into the main n-channel. Our results can be explained qualitatively if the 'mini-channel escape time constant' is long compared to the horizontal pixel shift time but short compared to the vertical row shift time. In our testing, the serial shift time was 22 μsec/pixel, much faster than the row shift time of 91 msec. We did not vary the clock patterns in our testing to investigate this hypothesis since the focus was on assessment of performance using flight timing.

---

[3] Biretta, J. *et al*., *Charge Transfer Efficiency in the WFPC2 CCD Arrays*, Paper 12.14 Presented at the 197th Meeting of the American Astronomical Society, January 2001.

[4] Gilliland, Ronald L., Goudfrooij, Paul and Kimble, Randy A., *Linearity and High Signal-to-Noise Performance of the STIS CCD*, Publications of the Astronomical Society of the Pacific, Vol. 111, August 1999.

[5] Kimble, Randy A., Goudfrooij, Paul and Gilliland, Ronald L. Radiation Damage Effects on the CCD Detector of the Space Telescope Imaging Spectrograph, Paper 85.02 Presented at the 195th Meeting of the American Astronomical Society, January 2000.

[6] Riess, Adam, *How CTE Affects Extended Sources*, Space Telescope Science Institute Instrument Science Report WFPC2 00-04, 28 September 2000.

The power-law decrease in CTE with decreasing signal level indicates that faint science targets will be most severely affected. A signal level dependent redistribution of charge will occur in star images and in the observed spatial brightness distributions of extended objects. Errors in stellar photometry, measured astrometric positions, and surface brightness observations will all increase over time as displacement damage accumulates in the CCD detector. Results from the ACS CCD ground test effort together with orbital experience from WFPC2 and STIS led to a program decision to add post-flash capability to the WFC and High Resolution Camera (HRC) CCD cameras. When integration on the target is complete, the focal plane is flashed with an LED light source to pre-fill the traps before readout begins. A post-flash system was chosen instead of a pre-flash system because post-flash maximizes the probability that the traps will remain filled as the image is clocked out. Post-flash does, however, entail a S/N penalty because of photon shot noise. The strategy for ACS is to use post-flash to ameliorate radiation damage only later in the lifetime of the instrument when charge transfer effects begin to significantly impact the quality of the science images.